Organic Electronics 27 (2015) 101–106

Contents lists available at ScienceDirect

Organic Electronics

journal homepage: www.elsevier.com/locate/orgel

Electrical control of the distributed feedback organic semiconductor laser based on holographic polymer dispersed liquid crystal grating

Zhihui Diao*, Lingsheng Kong, Li Xuan, Ji Ma

Changchun Institute of Optics, Fine Mechanics and Physics, Chinese Academy of Sciences, Changchun, 130033, China

ARTICLE INFO

Article history:
Received 7 August 2015
Received in revised form
5 September 2015
Accepted 9 September 2015
Available online 19 September 2015

Keywords:
Electrical control
Organic semiconductor laser
Holographic polymer dispersed liquid crystal grating

ABSTRACT

In this paper, we demonstrate the electrical control of the distributed feedback (DFB) organic semiconductor laser based on a holographic polymer dispersed liquid crystal (HPDLC) grating for the first time. The grating is fabricated on the top of the organic semiconductor film to act as an external feedback structure. Experimental results show that the lasing intensity can be decreased by increasing the external electric field, and the lasing wavelength exhibits a slight blue-shift of 1.4 nm during the modulation process, indicating a good stability. The modulated performances are attributed to the decreases in the refractive index modulation and average refractive index of the HPDLC grating respectively as a result of the field-induced liquid crystal reorientation. This study provides some new ideas for the improvement of DFB organic semiconductor laser to enable envisioned applications in laser displays and integrated photonic circuits.

1. Introduction

During the past decade, electrically controllable lasers have attracted a great deal of interest as the active laser sources for various applications including wavelength division multiplexing (WDM) [1], laser displays and integrated photonic circuits [2,3], because their lasing characteristics (e.g., lasing wavelength or energy) can be easily modulated by electric field. To achieve an electrically controllable laser, a promising and efficient way is to incorporate liquid crystal (LC) in the laser resonator cavity because the orientation of LC molecules with large anisotropy and their refractive indices can be modified by external electric field. Two kinds of LCs have been widely used in the electrically controllable lasers. One is the nematic LC which is often added in optical waveguide [4–7]. The field-induced LC rotation can easily change the waveguide properties, and thus the lasing characteristics. The other one is the cholesteric LC which can form a self-assembled helical structure and result in a photonic band gap [8]. The helical structure can be deformed by LC rotation, which leads to a modulation of lasing wavelength [9] or energy [10]. Among the LC-based controllable lasers, the active laser media are always chosen to be the laser dyes since they can easily blend with LC. However, the concentration quenching effect of dyes in the pure solid film severely limits their lasing efficiencies and thus the practical application [11]. Compared to the dyes, organic semiconductor materials, as the new generation of laser media, show three advantages [12,13] of a) stronger pump absorption and gain in the solid state, b) simpler processing to make thin film for laser structure and c) capability of charge transport which opens up the possibility of electrical pumping. These advantages enable the organic semiconductors great scientific interest and technological significance, and so much research has been reported on the organic semiconductor lasers [12–17]. However, few reports have been devoted to the electrical control of the laser emission from organic semiconductors.

In earlier works [18], we have demonstrated a distributed feedback (DFB) organic semiconductor laser based on a holographic polymer dispersed liquid crystal (HPDLC) grating acting as an external feedback structure. Stable single-mode transverse electric (TE)-polarized laser emission was obtained under optical pumping. The use of HPDLC grating empowered by one-step holography technique results in low-cost and simple fabrication, rapid and large-area device prototyping and capability of electrical control because of the introduction of LC [18–23]. In this paper, to the best of our knowledge, we report the electrical control of the DFB organic semiconductor laser based on a HPDLC grating for the first time. The experimental results show that the lasing intensity can be modulated by increasing the electric field from 0 to 15.0 V/μm.

* Corresponding author.
E-mail address: diaozh@ciomp.ac.cn (Z. Diao).

http://dx.doi.org/10.1016/j.orgel.2015.09.012
1566-1199/

During the modulation process, the lasing wavelength is found a good stability with a slight blue-shift of 1.4 nm. These results are attributed to the decreases in the refractive index modulation and average refractive index of the HPDLC grating respectively, which are induced by the reorientation of LC molecules under external electric field.

2. Experiments

Fig. 1 shows the schematic structure of the controllable DFB organic semiconductor laser. A HPDLC grating is located on the top of an organic semiconductor poly(2-methoxy-5-(2′-ethyl-hexyloxy)-p-phenylenevinylene) (MEH-PPV, Jilin OLED Material Tech.) film between two indium-tin-oxide (ITO)-coated glass substrates. To acquire that structure, an empty cell was pre-fabricated by combining one glass substrate coated with MEH-PPV and the other one with polyimide (PI) film to align LC molecules, which was rubbed unidirectionally parallel to z axis (Fig. 1) corresponding to the groove direction of HPDLC grating. The MEH-PPV film was formed by spin-coating in a xylene solution (6 mg/mL) and its thickness was fixed at 80 nm by selecting appropriate rotation speed. Mylar spacers with a thickness of 6 μm were placed between the two substrates to control the cell gap. Then a uniform mixture of HPDLC pre-polymer syrup, consisting of difunctional acrylate monomer phthalic diglycol diacrylate (PDDA, 54.6 wt%, Sigma–Aldrich), LC TEB30A (33.0 wt%, $n_o = 1.522$, $n_e = 1.692$, Slichem) and photo-initiators (12.4 wt%), was injected and diffused into the entire cell via capillary action in the dark. The refractive index of the pure polymer formed by monomer PDDA was measured to be 1.525 by Abbe refractometer. The detailed materials composition of the photo-initiators can be found elsewhere [4]. After that, the sample cell was exposed to an interference pattern created by two coherent s-polarized laser beams from a 532 nm Nd:YAG laser. A HPDLC grating with periodic alternating LC and polymer layers was obtained via photo-polymerization after 5 min exposure. The wavelength λ_{las} of the DFB laser emission is determined by the grating period Λ, the effective refractive index n_{eff} of laser mode and the Bragg order m [24]:

$$\lambda_{las} = \frac{2n_{eff}\Lambda}{m}. \quad (1)$$

Considering that the n_{eff} of the laser mode from our DFB structure was about 1.60 [18], the grating period was carefully chosen as 395.2 nm to generate a second-order DFB laser with a wavelength around 630 nm located in the gain spectrum of MEH-PPV [13].

To determine the LC molecules orientation in the HPDLC grating, s- and p-polarized lights at 633 nm, generated by a combination of a He–Ne laser and a polarizer, were incident on the grating at the Bragg angle to measure the diffraction efficiency during the grating forming process, as described earlier [25]. Here, we note some direction issues for clarity that the s-polarized light and TE light have the same polarization state parallel to z axis, while the polarization state of p-polarized light is parallel to y axis.

As an optical pumping source for laser measurements, a 532 nm Q-switched Nd:YAG pulsed laser with 8 ns pulse duration and 3 Hz repetition rate was used. A cylindrical lens was applied to focus the pumping laser onto the sample with an incident angle of 60° relative to the glass substrate. The pumping beam shaped by an adjustable slit was about 3 mm in length and 0.1 mm in width. Under optical pumping, laser emission from the sample due to the second-order DFB effect [12,14] was collected along the sample normal by a fiber-coupled spectrometer (resolution: 0.2 nm). Since the output intensity of the pulsed pumping laser was not stable, the laser emission spectrum was measured 10 times under each pumping condition and an average result was presented in this paper to minimize the error. A square-wave voltage of 1 KHz frequency was output by a signal generator and applied on the sample to control the DFB laser emission.

3. Results and discussion

To better understand the electrical controllable performance of the DFB organic semiconductor laser, the orientation of LC molecules in the HPDLC grating needs to be identified first. The HPDLC grating studied here consists of two parts [25]: one is the polymer matrix with some trapped LC molecules which are randomly aligned and not free to rotate by external electric field [26], and the other is the pure LC layer in which the LC molecules orientation has a significant effect on the diffraction efficiency of HPDLC grating. Since the refractive index of pure polymer n_p (1.525) is more closer to n_o (1.522) rather than n_e (1.692), a higher diffraction efficiency can be obtained for the probe light with a polarization state parallel to the long axis of LC molecule which "sees" a refractive index of n_e. Fig. 2 shows the real-time diffraction efficiency of the grating for the s- and p-polarized probe lights. When the HPDLC grating is achieved, the diffraction efficiency for s-polarization is 44% higher than the one for p-polarization of 3%, which suggests that the orientation of LC molecules is preferentially parallel to the s-polarization state, that is, the grating groove (z axis). It is worth noting that the LC molecules orientation obtained in this experiment is different from our previous report [25], in which the LC molecules orientation is parallel to the grating vector (y axis). The reason for

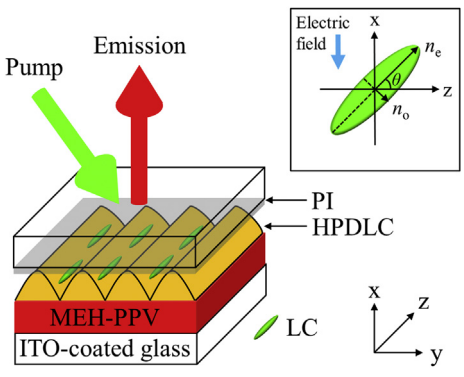

Fig. 1. Schematic structure of the DFB organic semiconductor laser. The inset shows the tilt angle θ of LC molecule under an electric field.

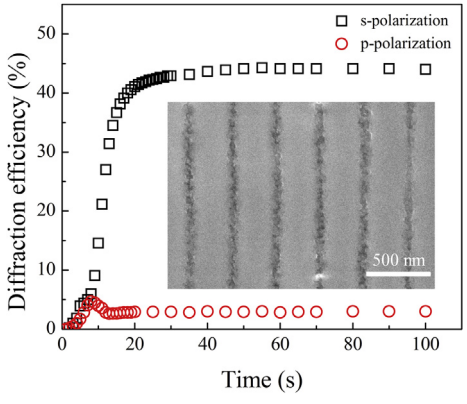

Fig. 2. The real-time diffraction efficiency for different polarizations. The inset shows the SEM image of the HPDLC grating.

the orientation change can be attributed to the PI film which can strongly influence the LC orientation [27]. Based on the obtained LC molecules orientation, the phase separation degree α, used to indicate the ratio of pure LC layers in the grating, is measured by a birefringence test [25] to be 13.8%. This result accords with the SEM measurement shown in the inset in Fig. 2, in which the dark region represents the pure LC layer.

When an external electric field is applied to the sample cell, the LC molecules in pure LC layer tend to align with their long axes into the field direction along x axis, so a rotation with a tilt angle θ in the x-z plane (the inset in Fig. 1) is induced. θ can be increased from 0° to 90° by increasing the electric field. Then the refractive index of pure LC layer n_{LC} for the emitted laser with TE polarization will be changed with the tilt angle as expressed by Ref. [28]:

$$n_{LC}(\theta) = \frac{n_o n_e}{\sqrt{n_o^2 \cos^2\theta + n_e^2 \sin^2\theta}}. \quad (2)$$

Accordingly, the average refractive index n_{ave} and refractive index modulation Δn of the HPDLC grating, which play significant roles on the DFB laser performance, can be modified. To quantitatively analyze the variation trends of n_{ave} and Δn, we reasonably assume that the HPDLC grating has two regions with same width of half the grating period [26,29]: one is the polymer matrix and the other is composed of the pure LC layer and partial polymer matrix. The refractive indices of the two regions can be expressed by:

$$n_a = \frac{0.67 \times n_p + (0.33 - \alpha) \times n_{iso}}{1 - \alpha}, \quad (3)$$

$$n_b = 2\alpha n_{LC}(\theta) + (1 - 2\alpha) n_a, \quad (4)$$

where n_{iso}, the average refractive index of LC, is 1.581. Then the average refractive index and refractive index modulation of the grating can be known:

$$n_{ave} = \frac{1}{2}(n_a + n_b) = \alpha n_{LC}(\theta) + (1 - \alpha) n_a, \quad (5)$$

$$\Delta n = \left|\frac{1}{2}(n_a - n_b)\right| = \alpha |n_a - n_{LC}(\theta)|. \quad (6)$$

Based on Eqs. (5) and (6), we can obtain the theoretical prediction of n_{ave} and Δn as a function of θ, as shown in Fig. 3. It can be seen that n_{ave} decreases monotonously with the increasing tilt angle. While for Δn, it decreases to zero when a critical angle (70.8°) is achieved, and after that critical angle it starts to increase.

In our DFB laser structure, the feedback mechanism for laser generation is only attributed to the pure index modulation, because the MEH-PPV film is planar and homogeneous which ensures the absence of gain modulation. As discussed in the coupled-wave theory of DFB laser [30], the coupling coefficient κ can be defined by:

$$\kappa = \frac{\pi \Delta n}{\lambda_{las}}, \quad (7)$$

which is related to the strength of the backward Bragg scattering and the amount of feedback power provided by the DFB structure. It can be obtained that a decreasing refractive index modulation will lead to a lower coupling effect of the DFB structure, and thus a higher lasing threshold and lower output lasing intensity [31,32]. Therefore, we can expect that the output intensity of the DFB organic semiconductor laser can be controlled by changing the refractive index modulation of HPDLC grating due to the rotation of LC molecules under an electric field.

A preliminary optical characterization of the DFB organic semiconductor laser was performed with no electric field applied on the sample cell. The obtained laser emission spectrum at a pumping energy density of 37.8 μJ/cm^2 is shown in Fig. 4. This spectrum exhibits a lasing peak at 629.9 nm with a spectral width of 0.7 nm, indicating single-mode (TE_0) laser emission from our sample. The inset in Fig. 4 presents the output lasing intensity as a function of pumping energy density, which implies the lasing threshold is about 16.5 μJ/cm^2.

The electrical control of the DFB organic semiconductor laser emission was investigated by applying an electric field on the sample cell, while the emission spectra were recorded simultaneously and shown in Fig. 5(a). The pumping energy density was measured to be 38.2 μJ/cm^2 and kept constant for all electric fields. When increasing the electric field from 0 to 15.0 V/μm, the lasing intensity can be controlled to decrease from 2100 to 92 (arb. unit). To further increase the electric field, the sample cell was broke down. The relationship between the lasing intensity and electric field is summarized in Fig. 5(b). It can be obtained that the lasing

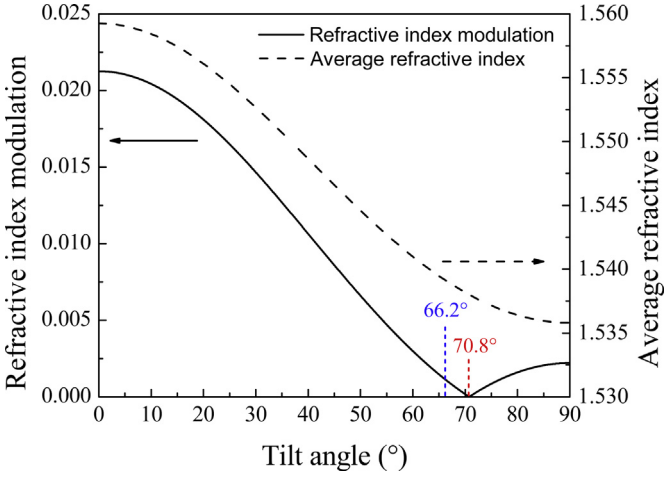

Fig. 3. Average refractive index and refractive index modulation of the grating as a function of tilt angle.

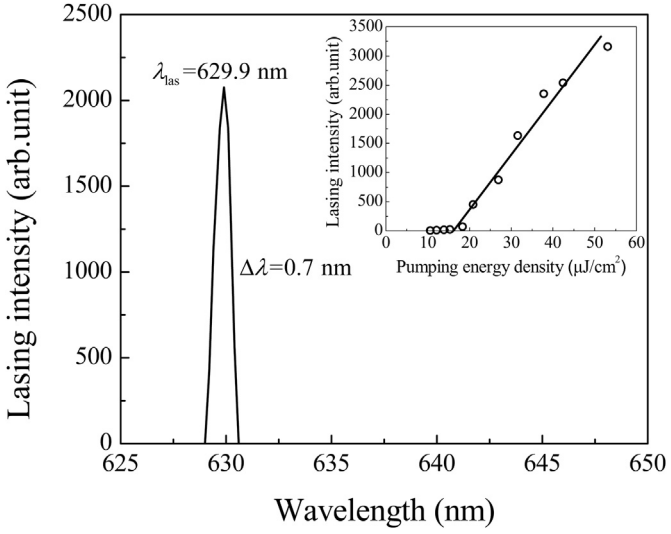

Fig. 4. Lasing spectrum at a pumping energy density of 37.8 μJ/cm^2. The inset shows the lasing intensity as a function of pumping energy density, indicating a threshold of 16.5 μJ/cm^2.

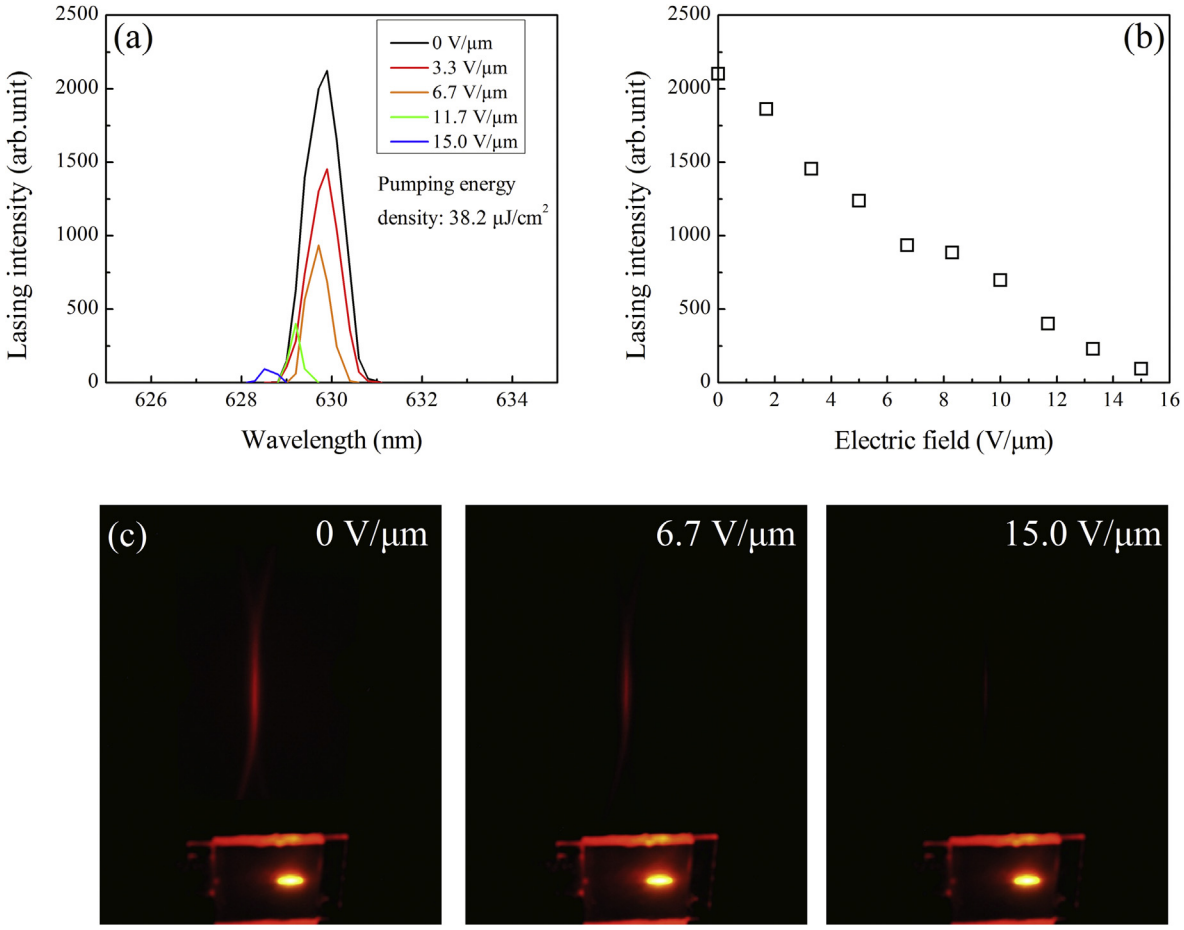

Fig. 5. (a) Lasing spectra of the DFB organic semiconductor laser under different electric fields. (b) The relationship between the lasing intensity and electric field. (c) Laser emission patterns under the electric fields of 0, 6.7, 15.0 V/μm.

intensity decreases linearly with the increasing electric field. Fig. 5(c) depicts a sequence of the laser emission patterns under different electric fields. In the absence of electric field, the laser emission pattern is red and bright, and confined in one direction perpendicular to the grating grooves which is typical for one-dimensional DFB laser [33,34]. As the electric field increases to 6.7 V/μm, the lasing energy is weakened obviously. And if the electric field rises continually to 15.0 V/μm, the lasing pattern is hard to recognize. Thus, as expected, the electrical control of the DFB organic semiconductor laser is achieved because the refractive index modulation Δn of the grating can be decreased as a result of the field-induced LC rotation. Furthermore, the lasing thresholds under different electric fields were measured and shown in Fig. 6. It can be found that the lasing threshold rises with the electric field. It is another sign of the decrease in Δn, because a lower Δn always leads to a higher lasing threshold [30,31].

There is still one problem should be explained that the variation trend of the lasing intensity does not follow the one of Δn as shown in Fig. 3. As the theoretical prediction of Δn, the lasing intensity should start to increase after decreasing to zero under a critical electric field that drives LC molecules to a tilt angle of 70.8°. However, that ideal result was not observed in experiment. To figure out that problem, we measured the tilt angle of LC molecules under the maximum electric field of 15.0 V/μm by a common method described earlier [4,28]. The measurement result shows that the maximum tilt angle that we can drive in the experiment is only about 66.2°, which is lower than the critical one of 70.8°. It can

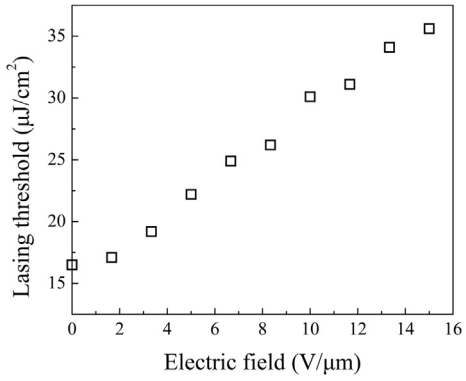

Fig. 6. The relationship between the lasing threshold and electric field.

be seen from Fig. 3 that the variation of Δn with tilt angle from 0° to 66.2° is monotonous, and that is the reason why the obtained lasing intensity varies monotonously with the electric field as well.

Moreover, the stability of the lasing wavelength during the control process is also investigated, as shown in Fig. 7(a). As the electric field is increased, the lasing wavelength is tuned to shorter wavelength and the spectral tuning is 1.4 nm. Compared to the lasing wavelength of 629.9 nm, the relative change of wavelength is only about 0.2%, which indicates a good stability. The slight blue-shift of lasing wavelength is attributed to the decreasing average

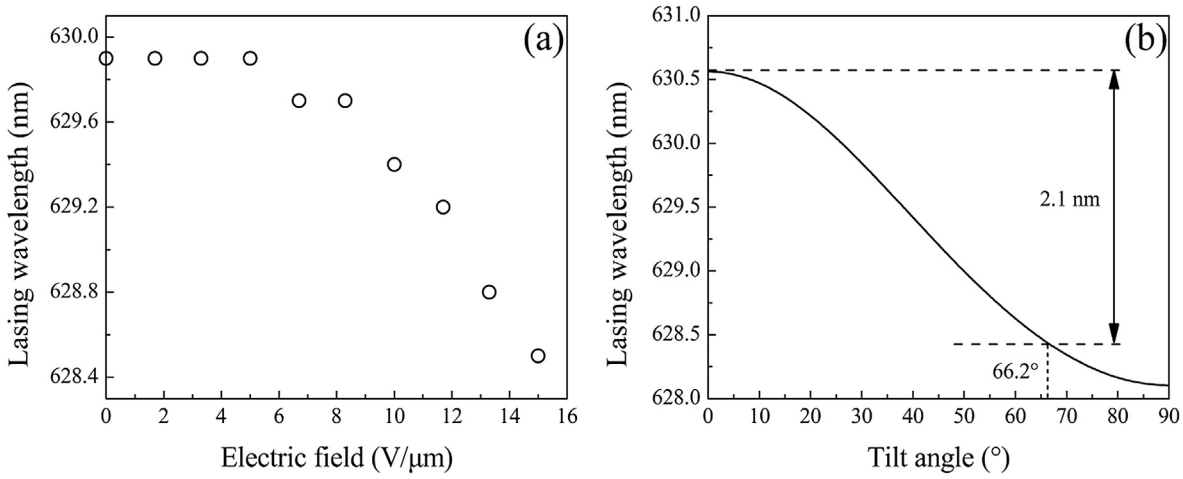

Fig. 7. (a) The relationship between the lasing wavelength and electric field. (b) Lasing wavelength as a function of tilt angle.

refractive index of grating (Fig. 3). In our DFB laser structure, an asymmetric slab waveguide is obtained in a form of grating/MEH-PPV/glass, in which the ITO layer with a thickness of 30 nm is too thin to be considered [4]. According to the waveguide theory [35], the waveguide equation for the TE light using the parameters from our DFB structure can be expressed by:

$$\frac{2\pi d}{\lambda_{las}}\sqrt{n_{ppv}^2-n_{eff}^2}=M\pi+\arctan\left(\sqrt{\frac{n_{eff}^2-n_{ave}^2}{n_{ppv}^2-n_{eff}^2}}\right)+\arctan\left(\sqrt{\frac{n_{eff}^2-n_{gla}^2}{n_{ppv}^2-n_{eff}^2}}\right), \quad (8)$$

where d is the MEH-PPV film thickness, M is the mode number, n_{ppv} and n_{gla} are the refractive indices of MEH-PPV film and glass substrate respectively. Through Eqs. (1), (5) and (8), the lasing wavelength as a function of LC tilt angle can be calculated and shown in Fig. 7(b). As the tilt angle is increased under an electric field, the refractive index of the cladding layer (HPDLC grating) decreases, which gives rise to a decrease in the effective refractive index of the laser mode in the core layer (MEH-PPV film), and thus the lasing wavelength. When the tilt angle increases from 0° to maximum 66.2°, the wavelength shift is about 2.1 nm. Compared to the experimental result 1.4 nm, the difference is acceptable considering that the resolution of the spectrometer used in experiment is only 0.2 nm.

4. Conclusions

In conclusion, we have demonstrated the electrical control of the DFB organic semiconductor laser based on a HPDLC grating. By determining the LC molecules orientation in HPDLC grating, we theoretically study the effect of electric-field-induced rotation of LC molecules on the average refractive index and refractive index modulation of the grating, which play essential roles on the final laser emission. Experimental results show that the output intensity of the DFB laser can be modulated by increasing the electric field, and the lasing wavelength exhibits a good stability with a relative change of 0.2%. These modulated lasing performances are attributed to the decreases in the refractive index modulation and average refractive index of the grating respectively. Therefore, we believe that the combination of the active optical device HPDLC grating and organic semiconductor materials will open a promising way to design active laser source and also widen the applications of organic semiconductors in the field of laser displays and integrated photonic circuits.

Acknowledgments

The authors would like to thank the support from the National Natural Science Foundation of China (grant No. 11174274).

References

[1] L.A. Coldren, G.A. Fish, Y. Akulova, J.S. Barton, L. Johansson, C.W. Coldren, Tunable semiconductor lasers: a tutorial, J. Light. Technol. 22 (2004) 193–202.
[2] D. Dragoman, M. Dragoman, Advanced Optoelectronic Devices, Springer, New York, 1998.
[3] F.J. Duarte, Tunable Laser Applications, CRC Press, New York, 2009.
[4] Z. Diao, W. Huang, Z. Peng, Q. Mu, Y. Liu, J. Ma, L. Xuan, Anisotropic waveguide theory for electrically tunable distributed feedback laser from dye-doped holographic polymer dispersed liquid crystal, Liq. Cryst. 41 (2014) 239–246.
[5] T. Matsui, M. Ozaki, K. Yoshino, Electro-tunable laser action in a dye-doped nematic liquid crystal waveguide under holographic excitation, Appl. Phys. Lett. 83 (2003) 422–424.
[6] R. Ozaki, T. Shinpo, K. Yoshino, M. Ozaki, H. Moritake, Tunable liquid crystal laser using distributed feedback cavity fabricated by nanoimprint lithography, Appl. Phys. Express 1 (2008) 012003.
[7] S. Klinkhammer, N. Heussner, K. Huska, T. Bocksrocker, F. Geislhöringer, C. Vannahme, T. Mappes, U. Lemmer, Voltage-controlled tuning of an organic semiconductor distributed feedback laser using liquid crystals, Appl. Phys. Lett. 99 (2011) 023307.
[8] Z. Zheng, B. Liu, L. Zhou, W. Wang, W. Hu, D. Shen, Wide tunable lasing in photoresponsive chiral liquid crystal emulsion, J. Mater. Chem. C 3 (2015) 2462–2470.
[9] Y. Inoue, H. Yoshida, K. Inoue, Y. Shiozaki, H. Kubo, A. Fujii, M. Ozaki, Tunable lasing from a cholesteric liquid crystal film embedded with a liquid crystal nanopore network, Adv. Mater. 23 (2011) 5498–5501.
[10] B. Liu, Z. Zheng, X. Chen, D. Shen, Low-voltage-modulated laser based on dye-doped polymer stabilized cholesteric liquid crystal, Opt. Mater. Express 3 (2013) 519–526.
[11] G. Kranzelbinder, G. Leising, Organic solid-state lasers, Rep. Prog. Phys. 63 (2000) 729–762.
[12] I.D.W. Samuel, G.A. Turnbull, Organic semiconductor lasers, Chem. Rev. 107 (2007) 1272–1295.
[13] M.D. McGehee, A.J. Heeger, Semiconducting (conjugated) polymers as materials for solid-state lasers, Adv. Mater. 12 (2000) 1655–1668.
[14] G. Heliotis, R. Xia, D.D.C. Bradley, G.A. Turnbull, I.D.W. Samuel, P. Andrew, W.L. Barnes, Blue, surface-emitting, distributed feedback polyfluorene lasers, Appl. Phys. Lett. 83 (2003) 2118–2120.
[15] Z. Diao, L. Xuan, L. Liu, M. Xia, L. Hu, Y. Liu, J. Ma, A dual-wavelength surface-emitting distributed feedback laser from a holographic grating with an organic semiconducting gain and a doped dye, J. Mater. Chem. C 2 (2014) 6177–6182.
[16] C. Kallinger, M. Hilmer, A. Haugeneder, M. Perner, W. Spirkl, U. Lemmer, J. Feldmann, U. Scherf, K. Mullen, A. Gombert, V. Wittwer, A flexible conjugated polymer laser, Adv. Mater. 10 (1998) 920–923.
[17] G.A. Turnbull, P. Andrew, M.J. Jory, W.L. Barnes, I.D.W. Samuel, Relationship

between photonic band structure and emission characteristics of a polymer distributed feedback laser, Phys. Rev. B 64 (2001) 125122.
[18] W. Huang, Z. Diao, Y. Liu, Z. Peng, C. Yang, J. Ma, L. Xuan, Distributed feedback polymer laser with an external feedback structure fabricated by holographic polymerization technique, Org. Electron. 13 (2012) 2307–2311.
[19] R. Caputo, L. De Sio, A. Veltri, C. Umeton, Development of a new kind of switchable holographic grating made of liquid-crystal films separated by slices of polymeric material, Opt. Lett. 29 (2004) 1261–1263.
[20] T.J. Bunning, L.V. Natarajan, V.P. Tondiglia, R.L. Sutherland, Holographic polymer-dispersed liquid crystals (H-PDLCs), Annu. Rev. Mater. Sci. 30 (2000) 83–115.
[21] Z. Diao, S. Deng, W. Huang, L. Xuan, L. Hu, Y. Liu, J. Ma, Organic dual-wavelength distributed feedback laser empowered by dye-doped holography, J. Mater. Chem. 22 (2012) 23331–23334.
[22] Z. Zheng, L. Zhou, D. Shen, L. Xuan, Holographic polymer-dispersed liquid crystal grating with low scattering losses, Liq. Cryst. 39 (2012) 387–391.
[23] Z. Zheng, F. Guo, Y. Liu, L. Xuan, Low threshold and high contrast polymer dispersed liquid crystal grating based on twisted nematic polarization modulator, Appl. Phys. B 91 (2008) 17–20.
[24] H. Kogelnik, C.V. Shank, Stimulated emission in a periodic structure, Appl. Phys. Lett. 18 (1971) 152–154.
[25] W. Huang, Y. Liu, Z. Diao, C. Yang, L. Yao, J. Ma, L. Xuan, Theory and characteristics of holographic polymer dispersed liquid crystal transmission grating with scaffolding morphology, Appl. Opt. 51 (2012) 4013–4020.
[26] J.J. Butler, M.S. Malcuit, M.A. Rodriguez, Diffractive properties of highly birefringent volume gratings: investigation, J. Opt. Soc. Am. B 19 (2002) 183–189.
[27] Y.T. Kim, S. Hwang, J.H. Hong, S.D. Lee, Alignment layerless flexible liquid crystal display fabricated by an imprinting technique at ambient temperature, Appl. Phys. Lett. 89 (2006) 173506.
[28] S.-T. Wu, D.-K. Yang, Fundamentals of Liquid Crystal Devices, John Wiley & Sons, 2006.
[29] W. Huang, S. Deng, W. Li, Z. Peng, Y. Liu, L. Hu, L. Xuan, A polarization-independent and low scattering transmission grating for a distributed feedback cavity based on holographic polymer dispersed liquid crystal, J. Opt. 13 (2011) 085501.
[30] H. Kogelnik, C.V. Shank, Coupled-wave theory of distributed feedback lasers, J. Appl. Phys. 43 (1972) 2327–2335.
[31] T.N. Smirnova, O.V. Sakhno, J. Stumpe, V. Kzianzou, S. Schrader, Distributed feedback lasing in dye-doped nanocomposite holographic transmission gratings, J. Opt. 13 (2011) 035709.
[32] G. Heliotis, R. Xia, G.A. Turnbull, P. Andrew, W.L. Barnes, I.D.W. Samuel, D.D.C. Bradley, Emission characteristics and performance comparison of polyfluorene lasers with one- and two-dimensional distributed feedback, Adv. Funct. Mater. 14 (2004) 91–97.
[33] S. Riechel, U. Lemmer, J. Feldmann, T. Benstem, W. Kowalsky, U. Scherf, A. Gombert, V. Wittwer, Laser modes in organic solid-state distributed feedback lasers, Appl. Phys. B Lasers Opt. 71 (2000) 897–900.
[34] C. Grivas, M. Pollnau, Organic solid-state integrated amplifiers and lasers, Laser Photonics Rev. 6 (2012) 419–462.
[35] K. Okamoto, Fundamentals of Optical Waveguides, Academic press, Burlington, 2010.